Energetics and Structures of Fluoro- and Chlorofluorocarbons in Zeolites: Force Field Development and Monte Carlo Simulations

Caroline F. Mellot*,† and Anthony K. Cheetham*,†,‡

Institut Lavoisier, UMR CNRS 173, Université de Versailles Saint-Quentin, 45 avenue des Etats-Unis, 78035 Versailles Cedex, France, and Materials Research Laboratory, University of California, Santa Barbara, California 93106

Received: September 18, 1998; In Final Form: January 26, 1999

Canonical Monte Carlo simulations on the adsorption of a series of fluoro-, chlorofluoro-, and hydrofluorocarbons (CF_4, CF_3Cl, CF_2Cl_2, $CFCl_3$, CHF_3) in siliceous Y and NaY zeolites have been performed and are compared with available calorimetric data on the same host−guest systems. A new force field for fluorocarbon-type molecules in zeolites has been developed, and our (*N,V,T*) simulations predict adsorption heats with good accuracy. Further insights into the key features of host−guest interactions are gleaned from the relative contributions of the short-range and electrostatic interactions to the total adsorption heats and the analysis of host−guest pair functions. In siliceous Y, host−guest interactions are driven primarily by F···$O_{zeolite}$ and Cl···$O_{zeolite}$ van der Waals interactions, and H···$O_{zeolite}$ hydrogen bonding in the case of hydrogen-containing fluorocarbons. When the fluorocarbon is adsorbed in a cation-containing zeolite, such as NaY, additional F···$Na_{zeolite}$ electrostatic interactions with Na cations of the supercage are clearly revealed and control the orientation of the sorbate molecules within the supercages. In addition, (*N,V,T*) simulations have enabled us to compare the behavior of CHF_3 with that of $CHCl_3$. The heats of adsorption at zero loading are very similar, but the relative contributions of the short-range and long-range interactions are inverted between the two systems, with the electrostatic term dominating in the case of the fluorocarbon.

Introduction

The adsorption of halocarbons in zeolites is attracting a great deal of attention at present due to its relevance to environmental issues concerning ozone-depleting chlorofluorocarbons (CFCs)[1] and the removal of chlorinated solvent residues from contaminated groundwater and soils.[2] For example, zeolite A and naturally occurring clinoptilolite have been shown to be efficient for the recovery of methyl chloride from the vent streams generated during the direct synthesis of methylchlorosilane.[3] Similarly, the basic NaX and NaY faujasites can be used to separate various hydrofluorocarbons (HFCs) during the manufacture of CFC substitutes.[4] In another context, hydrophobic silicalite (siliceous ZSM-5) is a good candidate for the sequestration of trichloroethylene from groundwater.[5,6] Our own interest in this area has so far focused on computer modeling and experimental studies of chlorocarbons in faujasite-type zeolites. Our recently developed force field predicts structural and thermochemical properties that are in excellent agreement with vibrational spectroscopy[7] and calorimetric data[8,9] for saturated and unsaturated chlorocarbons, such as chloroform and trichloroethylene, in a series of faujasites (siliceous Y, NaY, NaX).

In the present paper, we extend our force field development to some important fluorine-containing sorbates. Previous simulation work in this area has treated the cases of CFCs in siliceous zeolites using a generalized force field[10] or has used a nonatomistic model for the sorbate molecules.[11] There are very few experimental data concerning the adsorption of fluorocarbons and CFCs in zeolites and analogous microporous materials. Nevertheless, the heats of adsorption of several CFCs in deuterated H−Y zeolite have been estimated by calorimetric methods,[12] and isotherm measurements have been reported for dichlorodifluoromethane in Na−, K−, and Cs−Y zeolites.[13] In addition, the adsorption of CHF_2CHF_2 in NaY has been studied by synchrotron X-ray powder diffraction[14] and host−guest interactions of various hydrofluorocarbons in faujasite-type zeolites have been probed by NMR.[15] The present work considers the adsorption of some typical fluorinated molecules—CF_4, CF_3Cl, CF_2Cl_2 (CFC-12), $CFCl_3$ (CFC-11), and CHF_3—in siliceous faujasite and NaY. Our selection deliberately includes fluoro-, chlorofluoro-, and hydrofluorocarbons, thereby covering a wide range of halogen compositions and dipole moments (zero to 1.65 D). Prior to presenting our results, we describe our new potentiel model and explain the derivation of our force field parameters. We then compare (*N,V,T*) Monte Carlo simulations performed with the new force field with the calorimetric data available for the above host/guest systems from refs 12 and 13. The key features of fluorocarbon adsorption are rationalized through the analysis of the respective components of the total adsorption energies and the analysis of host−guest pair functions. As a further exploration of the intrinsic differences between the adsorption of the hydrochloro- and hydrofluorocarbons, we compare the coverage dependence of the adsorption heats of $CHCl_3$ and CHF_3 in zeolite NaY on the basis of their respective energetics and structural features.

Force Field Development

Fluorocarbon−Zeolite and Chlorofluorocarbon−Zeolite Interactions. The total host−guest interaction energy was taken as the sum of a short-range term, modeled with a (6-12) Lennard-Jones potential, and a long-range Coulombic term:

† Université de Versailles Saint-Quentin. E-mail: mellot@chimie.uvsq.fr.
‡ University of California. E-mail: cheetham@mrl.ucsb.edu.

10.1021/jp983776j CCC: $18.00
Published on Web 04/24/1999

$$E_{\text{Lennard-Jones}} = \sum_{ij}(A_{ij}/r^{12} - B_{ij}/r^6) = \sum_{ij}\epsilon_{ij}[(r^*_{ij}/r_{ij})^{12} - 2(r^*_{ij}/r_{ij})^6] \quad (1)$$

$$E_{\text{Coulombic}} = \sum_{ij} q_i q_j / r_{ij} \quad (2)$$

where A_{ij} is the repulsive constant, and B_{ij}, the dispersive constant, with $\epsilon_{ij} = B_{ij}^2/4A_{ij}$, $\sigma_{ij} = (A_{ij}/B_{ij})^{1/6}$ and $\sigma^*_{ij} = 2^{1/6}\sigma_{ij}$($\sigma_{ij}$ is the distance at which the energy becomes repulsive). We prefer providing values for (ϵ, r^*) parameters since they have direct physical and chemical meanings: r^* is the equilibrium separation distance between interacting pairs, and ϵ, the interaction energy at r^*. The A and B parameters can be readily calculated from r^* and ϵ using the above relationships. The host−guest induction energy was not included directly, though it is largely subsumed into our model through the Lennard-Jones parameters.

The short-range contributions of the zeolite host were calculated using only framework oxygens, plus Na cations in the case of NaY. The contributions of the Si and Al atoms were neglected since they have polarizabilities lower than that of oxygen and cannot be approached as closely by sorbate molecules. Short-range parameters between $(C,H)_{guest}$ atoms and $(O,Na)_{zeolite}$ atoms were taken from Monte Carlo simulation studies that reported good predictions of experimental adsorption heats of methane in various zeolites: faujasite, mordenite, and ZSM-5.[16] Short-range parameters between Cl_{guest} atoms and $(O,Na)_{zeolite}$ atoms were derived from our parameters of Ar in silicalite[17] (for details, see ref 7). Parameters for short-range interactions between F_{guest} atoms and $(O,Na)_{zeolite}$ atoms were obtained from our values for the Cl_{guest}−$(O,Na)_{zeolite}$ short-range interactions from ref 7. Since the direct estimation of the dispersion constant B_{ij} is difficult because of the variety of its empirical formulations, we use a simple and realistic approximation for deducing epsilons from one another: the $\epsilon_{F\cdots(O,Na)}$ parameters were obtained from the $\epsilon_{Cl\cdots(O,Na)}$ parameters by applying a decrease ratio of 1/4, thus accounting for the decrease in the atomic polarizability from Cl to F ($\alpha_F/\alpha_{Cl} \sim 1/4$); the $r^*_{F\cdots(O)}$ and $r^*_{F\cdots(Na)}$ parameters were deduced from our values for the $r^*_{Cl\cdots(O)}$ and $r^*_{Cl\cdots(Na)}$ parameters, respectively, so as to reflect the smaller size of F compared with Cl ($\Delta r^*_{Cl/F} = 0.4$ Å). Table 1 shows our zeolite−chlorofluorocarbon short-range parameters. We wish to stress that no fitting to experimental data on halocarbons was used in the derivation of these parameters.

Intermolecular interactions had to be taken into account for simulating the coverage dependence of the adsorption heat of CHF_3 in NaY. As above, the guest−guest parameters were derived from those reported in our work on chlorocarbons in faujasites,[8,9] by applying correction factors accounting for the differences between the Cl and F radii and polarizabilities (Table 2).

The zeolite structure was kept rigid and considered as semi-ionic using partial charges that are consistent with those in ab initio silicate potentials[18] and recent X-ray diffraction results.[19] We do not treat the possibility of cation migration, although Grey et al. have observed some redistribution in the system NaY/CF_2HCF_2H.[14] The zeolite hosts were modeled as follows: (i) siliceous faujasite, $Si_{192}O_{384}$ (Si:Al = ∞), was considered to be a good approximation for modeling the DY zeolite, with q(Si) = +2.4 and q(O) = −1.2; (ii) $Na_{48}(Si,Al)_{192}O_{384}$ (Si:Al = 3) was used for modeling the NaY zeolite, placing the 48 cations in sites I and II as described in our previous work.[7] Concerning the partial charges of the NaY model, an average T-atom (Al, Si) was considered for circumventing the difficulty of the disordered distribution of Al atoms in the framework, with q(Si,Al) = +2.15, q(O) = −1.2, and q(Na) = +1. Charges for the various guest molecules were derived from Hartree−Fock calculations (TURBOMOLE)[20] using a TZP basis set and fitting the electrostatic surface potential (EPS charges). Finally, the charges were scaled up or down if necessary in order to reproduce the experimental dipole moments. Table 3 gives the partial charges used in our work for all sorbate molecules.

All our Monte Carlo simulations used the Metropolis scheme in the (N,V,T) canonical ensemble, at a constant volume V and temperature T. All average energies were obtained over 10^6 iterations, after an equilibration period of 10^5 steps, with a short-range summation taken up to a cutoff radius of 12 Å and an Ewald summation regarding the electrostatic term. The software of the MSI Catalysis and Sorption Consortium was used for these simulations.[21]

TABLE 1: Parameters for Zeolite−Chlorofluorocarbon Short-Range Interactions in Siliceous Faujasite[a]

	ϵ_{ij} (K)	r^* (Å)
O···C	87.06	3.25
O···H	90.53	2.70
O···Cl[b]	165.4	3.43
O···F[b]	41.35	3.03
Na···C	13.24	3.69
Na···H	11.41	3.1
Na···Cl	212.48	2.9
Na···F	52.12	2.5

[a] The same parameters were used for siliceous faujasite and NaY, except for $\epsilon_{O\cdots Cl}$ and $\epsilon_{O\cdots F}$ (see note b). [b] In the case of NaY, the $\epsilon_{O\cdots Cl}$ and $\epsilon_{O\cdots F}$ parameters were increased by a ratio of 1.1 ($\epsilon_{O\cdots Cl}$ = 181.93 K, $\epsilon_{O\cdots F}$ = 45.48 K) accounting for the difference in framework polarizabilities between siliceous and cationic zeolites.[22]

TABLE 2: Parameters for Intermolecular Interactions Used for Chlorofluorocarbon Adsorption

	ϵ_{ij} (K)	r^* (Å)
C···C	25.86	3.75
C···Cl	55.65	3.79
C···F	13.91	3.39
C···H	26.73	3.36
Cl···Cl	119.8	3.82
Cl···H	57.53	3.39
Cl···F	34.67	3.70
F···F	29.7	3.02
F···H	14.38	2.99
H···H	27.63	2.96

TABLE 3: Estimated Partial Atomic Charges for Our Selection of Fluorocarbon Sorbates[a]

	charges			
sorbates	C	F	Cl	H
CF_4	0.800	−0.200		
CF_3Cl	0.614	−0.176	−0.086	
CF_2Cl_2	0.210	−0.086	−0.019	
$CFCl_3$	−0.039	−0.033	0.024	
CHF_3	0.719	−0.245		0.016
$CHCl_3$	−0.102		−0.026	0.18

[a] Partial charges of $CHCl_3$ are reported for comparison with CHF_3.

Results

Table 4 compares the experimental adsorption heats available for the five sorbates, CF_4, CF_3Cl, CF_2Cl_2, $CFCl_3$, and CHF_3, in DY and/or NaY zeolites,[12,13] with the values obtained from our (N,V,T) Monte Carlo simulations. The simulated adsorption heats

TABLE 4: Summary of Experimental and Computed Heats of Adsorption for Our Selection of Host−Guest Systems

				adsorption heat (kJ/mol)		internal energy (kJ/mol)[b]	
sorbate	zeolite	dipole (D)	temperature (K)	exp	simul	short-range term	long-range term
CF_4[a]	DY	0	423	*−12.4*[12a]	−12.2	−6.7	−2.0
CF_3Cl[a]	DY	0.5	423	*−21.5*[12b]	−18.5	−12.9	−2.1
CF_2Cl_2[a]	DY	0.51	423	*−25.3*[12a]	−23.0	−18.9	−0.6
			278		−24.6	−20.7	−1.6
	NaY		278	*−33.4*[13]	−29.1	−22.3	−4.4
$CFCl_3$[a]	DY	0.45	423	*−24.6*[12a]	−27.9	−24.2	−0.3
CHF_3	NaY	1.65	300	N/A	−45.8	−7.5	−35.8
$CHCl_3$	NaY	1.06	300	*−53.2*[8]	−48.8	−34.5	−11.8

[a] We compare our simulations with data reported in ref 12a. The same authors have published a second set of data in ref 12b, some of which are rather different from the ones in ref 12a. With the exception of CF_3Cl, which was believed to be inaccurate in ref 12a, we have compared our simulations with their original estimates. [b] An additional $-kT$ term (−2.3 kJ/mol at 278 K, −2.5 kJ/mol at 298 K, −3.5 kJ/mol at 423 K) has to be added to the short-range and long-range terms in order to give the total simulated adsorption heats.

were estimated at the zero coverage limit ($N = 1$ molecule per unit cell) and at the appropriate temperatures. In the following sections, we discuss the energetics of these adsorption processes and the location of the sorbate molecules.

Adsorption of Fluoro- and Fluorochlorocarbons (CF_4, CF_3Cl, CF_2Cl_2, $CFCl_3$). Our simulations capture the experimental heats of adsorption with good accuracy in both DY and NaY zeolites. To obtain further insights into the variations in the heats of adsorption from one host−guest system to another, the total adsorption heats were decomposed into their short-range and long-range components (Table 4). In addition, the pair functions (PFs) taken from our Monte Carlo simulations at zero loading were analyzed. In the following, the PF calculated over the solid for each pair of atoms shows the histogram of the content of successive shells out from the central atom, as a function of their radii. We discuss here the PFs for a selection of typical host−guest systems.

Concerning the adsorption of CF_4 in zeolite DY (at 423 K), the simulated and experimental adsorption heats are in very good agreement. The interaction is dominated by the contribution of the short-range term over electrostatic interactions, arising mainly from F···$O_{zeolite}$ van der Waals interactions. As expected, the contribution of the dispersive interactions to the total adsorption heat increases from CF_3Cl to CF_2Cl_2 and $CFCl_3$, in a given host and at a given temperature, following the sequence of the number of Cl atoms per sorbate molecule; this clearly results from the higher atomic polarizability of the Cl atoms in comparison with the F atoms. By contrast, the contribution of the electrostatic term to the total adsorption heat is quite small, whatever the sorbate, and follows no simple trend. The adsorption of fluorochlorocarbons in noncationic zeolite such as DY is therefore essentially driven by dispersive interactions between F and Cl atoms and framework oxygens. This is nicely illustrated by the Monte Carlo PFs in Figure 1, which show the occurrence of both F···$O_{zeolite}$ and Cl···$O_{zeolite}$ interactions in the case of CF_2Cl_2 in DY from our simulation at zero loading and 278 K. The PFs obtained for this system at 423 K showed the same features.

In the case of CF_2Cl_2 adsorption in NaY, the presence of extraframework cations gives rise to additional host/guest electrostatic interactions, increasing the electrostatic contribution by almost a factor of 3 compared with DY (see Table 4). This establishes the role of the dipole moment of the CFC molecule, and its interaction with the electric field generated by the structure, in the case of the more polar cation-containing zeolite. In this respect, the PFs relating to CF_2Cl_2 in NaY (Figure 2) reveal further details of the position of CF_2Cl_2 in NaY at 278 K, especially when compared to those in DY; while the features of the F···$O_{zeolite}$ and Cl···$O_{zeolite}$ PFs are very similar to those already obtained for CF_2Cl_2 in DY (Figure 1), new specific interactions are revealed between the Na cations and the CF_2Cl_2 molecules. Particularly noteworthy is the F···$Na_{zeolite}$ peak

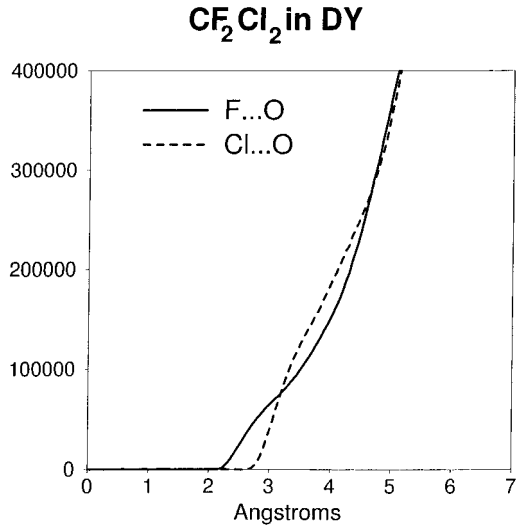

Figure 1. Pair functions for CF_2Cl_2 in DY, taken from our (*N,V,T*) Monte Carlo simulations at the zero coverage limit (1 molecule/unit cell) at 278 K. The PF calculated over the solid for each pair of atoms shows the histogram of the content of successive shells out from the central atom, as a function of their radii.

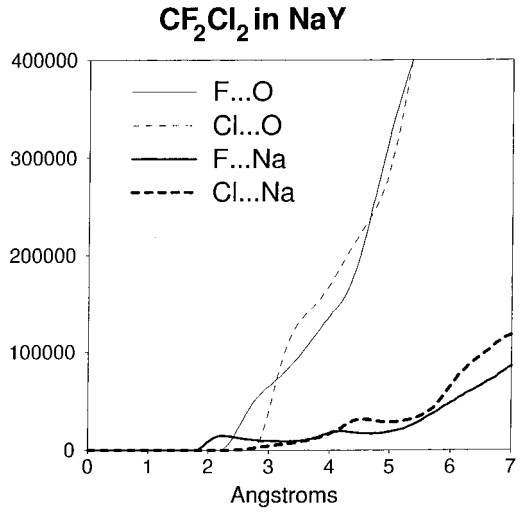

Figure 2. Pair functions for CF_2Cl_2 in NaY, taken from our (*N,V,T*) Monte Carlo simulations at the zero coverage limit (1 molecule/unit cell) at 278 K. Distinct features in the F···$Na_{zeolite}$ and Cl···$Na_{zeolite}$ PFs arise from electrostatic interactions.

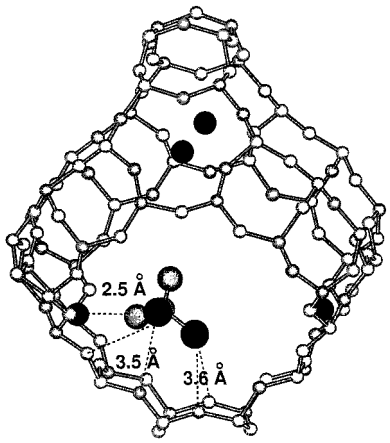

Figure 3. Adsorption site geometry for CF_2Cl_2 in NaY taken from the accepted configurations of the (*N,V,T*) Monte Carlo simulations, at the zero coverage limit and 278 K: (small black circles) Na cations in site SII, at the center of the 6-rings in the supercage; (large black circles) chlorine atoms of the CF_2Cl_2 molecule; (large gray circles) fluorine atoms of the CF_2Cl_2 molecule.

at 2.3 Å, which reflects the preferential interaction of the more negative fluorines with the sodium cations. This is underlined in Figure 3, where we show a typical example for an adsorption site geometry for CF_2Cl_2 in NaY taken from the (*N,V,T*) Monte Carlo simulations. It shows the main host−guest interactions expected from our simulations. The attraction of one of the fluorine atoms toward the Na cations in sites SII is clearly visible, while the chlorines interact predominantly with the framework oxygens with typical $Cl\cdots O_{zeolite}$ distances of ∼3.5 Å. These factors control the orientation of the molecule in the supercage. The $F\cdots Na_{zeolite}$ interactions are an important feature of the model proposed by Grey et al. for the system NaY/CF_2-HF_2H[14] and are shown to be of importance for various hydrofluorocarbons in NaY by $^{19}F/^{23}Na$ cross-polarization NMR.[15]

Adsorption of Hydrofluorocarbon. Comparison between $CHCl_3$ and CHF_3 in NaY. The CHF_3 molecule is of special interest as a model sorbate since it contains a hydrogen atom and has a high dipole moment (1.65 D). We discuss below our Monte Carlo predictions for CHF_3 adsorption in NaY in comparison with those of $CHCl_3$, its hydrochlorocarbon analogue.[7,8]

At the zero coverage limit and 300 K, the simulated adsorption heat for CHF_3 in NaY is 45.8 kJ/mol (Table 3), very close to that of $CHCl_3$ (48.8 kJ/mol)[8] in NaY. However, the striking difference between CHF_3 and $CHCl_3$ adsorption in NaY is that the relative contributions of the dispersive and electrostatic interactions are exactly reversed, fortuitously leading to similar adsorption heats for both sorbates (Table 4). The predominance of the electrostatic interactions in the CHF_3/NaY system is easily understood on the basis of the higher dipole moment of CHF_3 (1.65 D) compared to that of $CHCl_3$ (1.06 D). Equally, the enhanced role of the short-range interactions in $CHCl_3$/NaY is consistent with the discussion in the previous section.

To further explore the differences between CHF_3 and $CHCl_3$ adsorption in NaY, we have compared the variations of the adsorption heats of the two systems with sorbate loading. To that end, a series of (*N,V,T*) simulations were performed on the CHF_3/NaY system, varying the number of guest molecules, *N*, from a single molecule per unit cell up to 30 molecules per unit cell. Figure 4 shows the loading dependence of the CHF_3 adsorption heat obtained from our simulations (300 K) and its

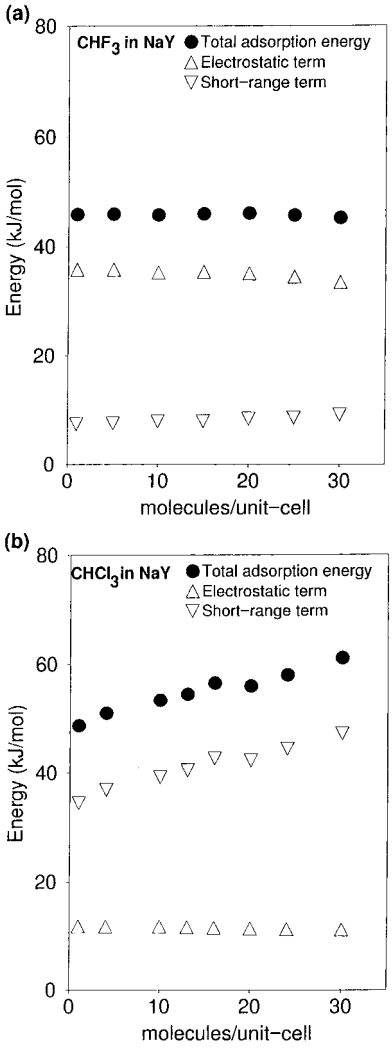

Figure 4. (a) Heats of adsorption of CHF_3 in NaY at 300 K estimated from our (*N,V,T*) Monte Carlo simulations as a function of loading, shown with their short-range and long-range contributions. (b) For comparison, the heats of adsorption of $CHCl_3$ in NaY at 300 K estimated from our (*N,V,T*) Monte Carlo simulations are shown as a function of loading, with their short-range and long-range contributions.[8]

decomposition into the short-range and long-range components; the loading dependence of $CHCl_3$ adsorption heat in NaY (300 K) is shown for comparison. Interestingly, the CHF_3 adsorption heat shows a flat profile with loading as a consequence of the constancy of both the electrostatic and dispersive terms. This is in constrast with $CHCl_3$, where the increase of the total adsorption heat with loading arises from intermolecular attraction, of a purely dispersive nature, between chloroform molecules.[8] This difference between the loading dependences of CHF_3 and $CHCl_3$ again relies on the much lower atomic polarizability of fluorine in comparison with chlorine, so that the flat profile observed with CHF_3 can be interpreted as in terms of adsorption of molecules on a set of independent, noninteracting sites.

Figure 5 shows the PFs of CHF_3 in NaY obtained from our Monte Carlo simulations at zero loading and 300 K. The position of CHF_3 in NaY shows the following key features: (i) in common with the above fluoro- or fluorochlorocarbons (CF_4, CF_3Cl, CF_2Cl_2, $CFCl_3$), host−guest interactions are driven by $F\cdots O_{zeolite}$ dispersive interactions and $F\cdots Na_{zeolite}$ electrostatic interactions, with distinctive peaks at 2.8 and 2.1 Å, respectively; (ii) in common with hydrochlorocarbons, such as chloroform[8]

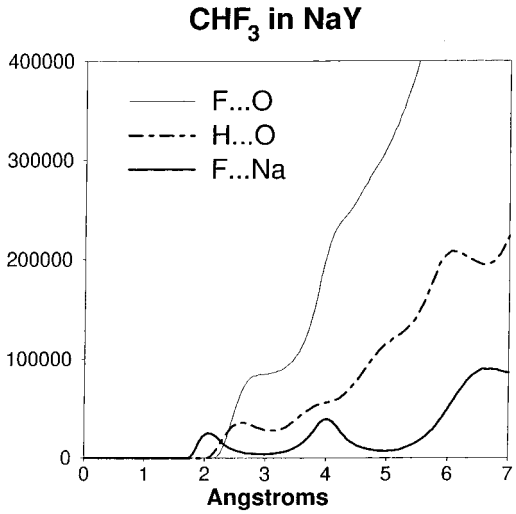

Figure 5. Pair functions for CHF_3 in NaY, taken from our Monte Carlo simulations at the zero coverage limit (1 molecule/unit cell) at 278 K. Distinct additionnal features in the $H\cdots O_{zeolite}$ figures arise from hydrogen bonding.

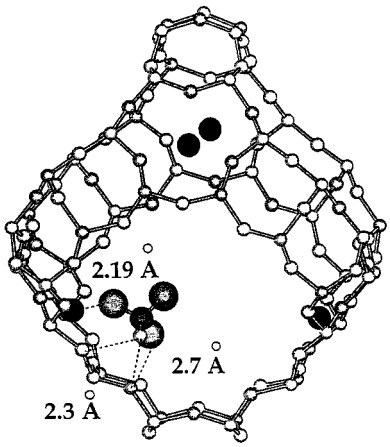

Figure 6. Adsorption site geometry for CHF_3 in NaY taken from the accepted configurations of the (*N,V,T*) Monte Carlo simulations at 300 K.

and trichloroethylene,[9] clear evidence of $H\cdots O_{zeolite}$ hydrogen bonding is observed at ~2.6 Å. This feature is again in line with the recent NMR study of Grey et al. on various HFCs in zeolite NaY.[15] Figure 6 shows a typical adsorption site geometry for CHF_3 in a supercage, taken from our (*N,V,T*) simulations; it reveals both of the above features.

Conclusion

As shown by the very good agreement between experiment and simulation for our selection of fluoro-, fluorochloro-, and hydrofluorocarbon/zeolite systems, our results provide strong validation of our force field for describing the adsorption of fluorine-containing halocarbons into noncationic and cationic zeolites. Furthermore, the findings shed considerable light, in line with chemical intuition, on the factors involved in the host−guest interactions in these systems, and the intrinsic differences between fluorocarbon and chlorocarbon adsorption processes. It now remains for us to extend this protocol to other host systems with different channel dimensions, such as the MFI architecture.

Acknowledgment. This work was supported by the U.S. Department of Energy under grant No. DE-FG03-96ER14672. A.K.C. thanks the Fondation de l'Ecole Normale Supérieure and the Région de l'Ile de France for a Chaire Internationale de Recherche, Blaise Pascal.

References and Notes

(1) Manzer, L. E.*Science* **1990**, *249*, 31.
(2) Hutchings, G. J.; Heneghan, C. S.; Ian, D. Hudson; Taylor, S. H. *Nature* **1996**, *384*, 341. See also: Mukhopadhyay, H.; Moretti, E. C. *Current and Potential Future Industrial Practices for Reducing and Controlling Volatile Organic Compounds*; American Institute of Chemical Engineers, Center for Waste Management: New York, 1993.
(3) Zarchy, A. S.; Maurer, R. T.; Chao, C. C. U.S. Patent No. 5 453 113, 1994.
(4) Corbin, D. R.; Mahler, B. A. World Patent, W. O. 94/02440, 1994.
(5) Alvarez-Cohen, L.; McCarty, P. L.; Roberts, P. V. *Environ. Sci. Technol.* **1993**, *27*, 2141.
(6) Weber, G.; Bertrand, O.; Fromont, E.; Bourg, S.; Bouvier, F.; Bissinger, D.; Simonot-Grange, M. H. *J. Chim. Phys.* **1996**, *93*, 1412.
(7) Mellot, C. F.; Davidson, A. M.; Eckert, J.; Cheetham, A. K. *J. Phys. Chem.* **1998**, *102*, 2530.
(8) Mellot, C. F.; Cheetham, A. K.; Harms, S.; Savitz, S.; Gorte, R. J.; Myers, A. L. *J. Am. Chem. Soc.* **1998**, *120*, 5788.
(9) Mellot, C. F.; Cheetham, A. K.; Harms, S.; Savitz, S.; Gorte, R. J.; Myers, A. L. *Langmuir* **1998**, *14*, 6728.
(10) (a) George, A. R.; Freeman, C. M.; Catlow, C. R. A. *Zeolites* **1996**, *17*, 466. (b) Parise, J. B.; Abrams, L.; Calabrese, J. C.; Corbin, D. R.; Newsam, J. M.; Levine, S.; Freeman, C. *Stud. Surf. Sci. Catal.* **1995**, *98*, 248.
(11) Clark, L. A.; Gupta, A.; Snurr, R. Q. *J. Phys. Chem.* **1998**, *102*, 6720.
(12) (a) Stach, H.; Sigrist, K.; Radeke, K.-H.; Riedel, V. *Chem. Tech.* **1994**, *46*, 278. (b) Stach, H.; Sigrist, K.; Radeke, K.-H.; Riedel, V. *Chem. Tech.* **1995**, *47*, 55.
(13) Kobayashi, S.; Mizuno, K.; Kushiyama, S.; Aizawa, R.; Koinuma, Y.; Ohuchi, H. *Ind. Eng. Chem. Res.* **1991**, *30*, 2340.
(14) Grey, C. P.; Poshni, F. I.; Gualtieri, A. F.; Norby, P.; Hanson, J. C.; Corbin, D. R. *J. Am. Chem. Soc.* **1997**, *119*, 1981.
(15) (a) Grey, C. P.; Corbin, D. R. *J. Chem. Phys.* **1995**, *99*, 16821. (b) Lim, H. P.; Grey, G. P. *Chem. Commun.* **1998**, 2257.
(16) Yashonath, S.; Thomas, J. M.; Nowak, A. K.; Cheetham, A. K *Nature* **1988**, *331*, 601. Smit, B.; den Ouden, C. J. J. *J. Phys. Chem.* **1988**, *92*, 7169.
(17) Mellot, C.; Lignières, J. *Mol. Simul.* **1997**, *18*, 349.
(18) Kramer, G. J.; Farragher, N. P.; van Beest, B. W. H.; van Santen, R. A. *Phys. Rev. B* **1991**, *43*, 5068.
(19) Ghermani, N. E.; Lecomte, C.; Dusausoy, Y. *Phys. Rev. B* **1996**, *53*, 5231.
(20) Ahlrichs, R.; Bär, M.; Häser, M.; Horn, H.; Kölmel, C. *Chem. Phys. Lett.* **1989**, *162*, 165. TURBOMOLE is distributed by MSI, 9685 Scranton Rd., San Deigo, CA 92121-277.
(21) *Catalysis 4.0 Software Suite*, Version 3.2; MSI: San Diego, CA.
(22) Pellenq, R. J. M.; Nicholson, D. *J. Chem. Soc., Faraday Trans.* **1993**, *89*, 2499.